



Contents lists available at ScienceDirect



Catalysis Today

journal homepage: www.elsevier.com/locate/cattod

Fe/EuroPh catalysts for limonene oxidation to 1,2-epoxylimonene, its diol, carveol, carvone and perillyl alcohol

Jacek Młodzik^a, Agnieszka Wróblewska^{b,*}, Edyta Makuch^b, Rafał J. Wróbel^a, Beata Michalkiewicz^{a,**}

^a West Pomeranian University of Technology, Institute of Chemical and Environment Engineering, Pulaskiego 10, PL 70-322 Szczecin, Poland

^b West Pomeranian University of Technology, Institute of Organic Chemical Technology, Pulaskiego 10, 70-322 Szczecin, Poland

ARTICLE INFO

Article history:

Received 28 August 2015

Received in revised form

11 November 2015

Accepted 14 November 2015

Available online xxx

Keywords:

Activated carbon

Iron catalysts

Limonene oxidation

Hydrogen peroxide

Tert-butyl hydroperoxide

Fe₃O₄

ABSTRACT

The catalysts in the form of an activated carbon EuroPh supported Fe were prepared and characterized structurally and chemically by XRD, nitrogen sorption, FESEM, EDX, and ICP-AES methods. The active phase was magnetite Fe₃O₄. The concentration of Fe in the catalysts was equal to 0.68, 1.32, 2.64 wt%. The catalytic activity of the obtained catalysts was examined in limonene oxidation with hydrogen peroxide and *tert*-butyl hydroperoxide as oxidants. The studies were carried out in a batch reactor. The catalytic activity of the recovered catalysts was also tested. The research showed that all from the studied catalysts were active in the limonene oxidation. As a result of limonene oxidation the following products were mainly obtained: 1,2-epoxylimonene diol, carveol, carvone and perillyl alcohol – products with a great importance. The reused catalysts were characterized by considerably lower activity in the limonene oxidation than in the first run, especially when the oxidation was performed with *t*-butyl hydroperoxide.

© 2015 Elsevier B.V. All rights reserved.

1. Introduction

The oxidation of limonene is very important and carefully studied reaction because it allows to obtain various value-added products, such as: limonene oxides, carvone, carveol, perillyl alcohol, menthol, α -terpineol and other. Carvone and carveol are important compounds for food and cosmetics industry [1]. Epoxides are important intermediates for organic synthesis, and can be transformed into various products for example ketones [2].

Limonene is the main component of citrus oil (the content of limonene in the oil reaches about 97%), obtained from the waste orange peels. This natural substrate is easily available and low-priced. Limonene can undergo either allylic oxidations or epoxidation reactions. Allylic oxidation is a reaction involving free radicals and is more likely to occur when the oxidizing metallic species is an intermediate in a low oxidation state [3]. Epoxide

formation is usually related to the use of oxometallic species [4]. However, both reactions have been shown to be competitive [5].

The following catalysts containing transition metal ions effectively catalyzed the limonene epoxidation: cobalt doped mesoporous silica templated by reed leaves, zeolite-Y entrapped-doxovanadium(IV) complexes, titanium-amine functionalized silica, indenyl molybdenum(II) tricarbonyl complex, mesoporous titanium-silicate Ti-MMM-2, anchoring manganese salen complexes on MCM-41 anchored, anchoring manganese acetylacetone complex on MCM-41, and V₂O₅/TiO₂ [6–13]. Clean oxidation of limonene using hydrogen peroxide under mild conditions is still a challenge in catalysis. We have found that iron is very interested as active phase.

Bartoli et al. [14] investigated catalytic properties of new iron(III) β -polynitroporphyrins in the oxidation of hydrocarbons. The iron porphyrin bearing five β -nitro groups was the best catalysts for oxidation of limonene by H₂O₂ or iodosylbenzene in CH₂Cl₂–MeCN serving as solvent. As products: 1,2-epoxylimonene, 8,9-epoxylimonene, carveol, and carvone were obtained. The highest yield (35%) was achieved for 1,2-epoxylimonene in the presence of iodosylbenzene as the oxidant.

Naróg et al. [15] investigated the oxidation of limonene by oxygen using as the catalysts Fe(II) and Fe(III) bis-2,2'-bipyridine complexes in acetonitrile. Moreover, in these studies

* Corresponding author. Tel.: +48 91 4494875; fax: +48 91 4494365.

** Corresponding author. Tel.: +48 91 4494875/+48 91 4494730; fax: +48 91 4494365/+48 91 4494686.

E-mail addresses: Agnieszka.Wroblewska@zut.edu.pl (A. Wróblewska), Beata.Michalkiewicz@zut.edu.pl (B. Michalkiewicz).

the gaseous oxygen was used as oxidant. After the reaction time of 24 h and at the temperature of 23 °C, the main products were: carvone (the yield of 4.5 mol%), carveol (the yield of 2.3 mol%), 1,2-epoxylimonene (the yield of 4.2 mol%), perillyl aldehyde (the yield of 2.3 mol%), and perillyl alcohol (the yield of 0.3 mol%). The highest limonene conversion was equal to 13.6 mol%.

Caovilla et al. [16] described catalyst involving covalently attached vanadium to modified Fe₃O₄ through a tetra-dentate Schiff base ligand for trans-2-hexene-1-ol, geraniol, limonene and 1-octene-3-ol epoxidation. The substrate was dissolved in chloroform. Diteriary butyl peroxide was used as the oxidant. The conversion of limonene after 4 h was 50 mol%. The 8,9-epoxylimonene, limonenone, limonene epoxide diol were obtained with selectivity of 62 mol%, 19 mol%, and 19 mol%, respectively.

The complex [Fe^{III}(bis(2-pyridylmethyl)-1,4-pirazoil)Cl(μ-O)Fe^{III}Cl₃] exhibited the catalytic activity towards limonene, β-pinene and α-pinene oxidation by hydrogen peroxide in acetonitrile as the solvent [16]. During oxidation twenty six products were obtained, but the main products were: carvone, carveol and limonene dioxide.

Skobelev et al. [17] applied 14,28-[1,3-diiminoisoindolinato] phthalocyaninatoiron(III) as the catalyst for the oxidation of a large range of olefins using H₂O₂ in MeCN as the solvent. The 1,2-epoxide, 8,9-epoxide, bis-epoxide were obtained with selectivity of 55 mol%, 30 mol% and 10 mol%, respectively, at the limonene conversion of 72 mol%.

The catalytic ability of Mn(III), Fe(III) and Co(III) complexes with TMePP-5,10,15,20-tetra(4-methoxyphenyl)porphyrin encapsulated within the pores of zeolite-Y [18] in the limonene oxidation by hydrogen peroxide was investigated by Madadi and Rahimi. In the oxidation ammonium acetate was applied as the co-catalyst and acetonitrile as the solvent. The highest limonene conversion equal to 81 mol% was achieved when catalyst containing Fe(III) was applied. The main products were 1,2-epoxylimonene and 8,9-epoxy-*p*-menth-1-ene. The selectivity these products was equal to 64 mol% and 36 mol%, respectively.

Hasan et al. [19] developed method of olefins epoxidation by combining FeCl₃·6H₂O as catalyst and 1-methylimidazole as the co-catalyst. In this reaction acetone was applied as the solvent. Hydrogen peroxide served as the terminal oxidizing agent. Such catalyst system was investigated for epoxidation of (+) and (-) limonene at the temperature of 62 °C and during the reaction time of 19–21 h. The conversion of the substrates was about 90 mol%, and limonene oxide was obtained with 63 and 83 mol% selectivity, respectively.

Herein we report the application of Fe₃O₄/activated carbon catalysts for limonene oxidation by hydrogen peroxide and *t*-butyl hydroperoxide (TBHP) in methanol as the solvent. In contrast to the above described complicated catalyst systems, we propose very simple and cheap catalysts. The utilization of such simple non-halogenated catalysts is desirable from an environmental point of view. The use of methanol as the solvent is a prospective advantage over other typical solvents such as: costly *tert*-butyl and *tert*-amyl alcohols, carcinogenic dichloromethane, and toxic acetonitrile. From economic and ecological point of view hydrogen peroxide is the preferred oxidant because it is cheap, easy to handle and water is produced as the only by-product of its transformation [20]. The main aim of this work was examination the activity of the obtained Fe/EuroPh catalysts in the oxidation of limonene, describing the main products of this oxidation taking into account the applied oxidants (H₂O₂ or TBHP) and testing the possibility of reusing of these catalysts.

2. Material and methods

2.1. Materials

For the synthesis of the catalysts iron(III) nitrate nonahydrate (Fe(NO₃)₃·9H₂O) obtained from Sigma-Aldrich Inc. and activated carbon EuroPh (EP) kindly supplied by Gryfskand Sp. zo.o. Hajnówka, Poland were applied.

2.2. Preparation of the catalysts

The activated carbon EuroPh (1.5 g) was mixed with the aqueous solution of Fe(NO₃)₃·9H₂O (0.0745 g and 0.1459 g and 0.2973 g in 10 cm³ H₂O) and left for 1 h under magnetic stirring. The resulting suspension was treated by the sonication for 1 h. The excess of water was evaporated at the temperature of 100 °C for 2 h. The sample was then calcinated at the temperature of 550 °C in tubular oven in a nitrogen flow. Activated carbons supported Fe₃O₄ and containing 0.68, 1.32 and 2.64 wt% of Fe were obtained. The iron content in the filtrate was measured by ICP-AES method (see Section 2.3.4). The catalysts were labeled as mEP where "m" refers to the mass percentage concentration of Fe. For example, a sample labeled as 0.68EP implies that the sample contains 0.68 wt% of Fe.

2.3. Catalysts characterization

2.3.1. X-rays diffraction analysis

The XRD patterns were recorded using PANalytical X-ray, Philips Analytical diffractometer with Cu Kα radiation ($\lambda = 1.5418 \text{ \AA}$). The angular speed was 0.033°/s with 0.02° step, from 10° to 90° at 2θ. A dried samples of the catalyst were grinded using an agate mortar and pestle. The spectra were analyzed using XPert High-Store diffraction software. The values of interlayer spacing (d), stack height (L_c), width (layer diameter) (L_a), effective dimension (L) of crystallites and average number of layers per stack (n_l) were calculated on the basis of XRD results.

The peak position and the half maxima of the peak positions of the (0 0 2), (1 0 0) and (1 1 0) band were applied to calculate the L_c and L_a using the Scherrer's equation [21]:

$$L_{c,a} = \frac{K \cdot \lambda}{(\beta_{c,a} - \beta_{0c,a}) \cdot \cos(\theta_{c,a})}$$

where K is the shape factor equal to 0.89 [22,23] and 1.84 [24] for L_c and L_a , respectively, λ is the Cu Kα wavelength, θ is the Bragg angle, β_{0c} and β_{0a} are the instrumental line broadening at θ_c and θ_a found experimentally, β_c and β_a are the full width at half height of the diffraction peaks.

The crystallite size L_c was obtained from the 0 0 2 band. The average layer diameter, L_a was obtained from the (1 0 0) and (1 1 0) bands.

The interlayer spacing was calculated from Bragg's law, from the peak position of the (0 0 2) band:

$$d = \frac{n \cdot \lambda}{2 \cdot \sin(\theta)}$$

where $n = 1$

The effective dimension L of the microcrystallites can be written as [25]:

$$L = \sqrt[2]{\frac{\pi}{4} L_a^2 L_c}$$

The average number of layers per stack was calculated on the basis of

$$n_l = \frac{L_c}{d}$$

The crystallite size of Fe_3O_4 was calculated using Scherrer's equation on the basis of three peaks (35.40° , 57.00° , 62.58°).

2.3.2. Specific surface area and pore structure analysis

Nitrogen sorption experiments were carried out using volumetric gas sorption instrument Quadsorb evo, Quantachrome. Before analysis, samples were outgassed at 250°C and at 1×10^{-6} bar during 16 h. The specific surface area (S_{BET}) was measured by means of BET (Brunauer–Emmett–Teller) equation applied in the relative pressure range of 0.03–0.3. The total pore volume (TPV) was calculated on the basis of the amount of nitrogen adsorbed at the highest relative pressure. Micropore volume (MPV) was estimated by Density Functional Theory method.

2.3.3. The Field Emission Scanning Electron Microscopy (FESEM) and Energy Dispersive Spectrometer (EDS) analysis

The micrographs and X-rays spectra were obtained using Ultra-High Resolution Field Emission Scanning Electron Microscope (UHR FE-SEM Hitachi SU8020) equipped with the Secondary Electron (SE) detectors, four quadrant Photo-Diode Backscattered Electron Detector (PD-BSE) and Energy Dispersive Spectroscopy system. Carbon tape was used for mounting powder catalyst. The micrographs were obtained with an acceleration of 15 kV. The X-ray spectra were taken with an acceleration of 20 kV.

The four quadrant photo-diode backscattered electron detector was used to generate compositional and crystallographic contrast images. The images obtained using PD-BSE detectors provide direct information on the distribution of heavier elements presented on the surface. Iron particles distribution observations were performed using the PD-BSE detector via electron channeling contrast imaging.

2.3.4. Determination of iron content by the Inductively Coupled Plasma-Atomic Emission Spectrometry (ICP-AES) method

Determination of iron concentration was investigated by the ICP-AES method. Iron was extracted using boiling hydrochloric acid. The samples (about 0.1 g) were treated by 50 ml of concentrated HCl (36 wt%) and heated to boiling point. After cooling, water was added up to 100 ml in a volumetric flask. The solid powder of carbon was removed by filtration. The iron content in the filtrate was measured by ICP-AES method.

2.4. Epoxidation method

In the oxidation of limonene the following reactants were used: R(+)-limonene (97%, Sigma), hydrogen peroxide (60 wt% water solution, Chempur), *t*-butyl hydroperoxide–TBHP (5.5 M solution in decane, Fluka) and methanol (analytical grade, Chempur).

The oxidation of limonene was carried out at the temperature of 70°C and in the range of the reaction time from 0.5 h to 48 h. The other parameters were as follows: the molar ratio of limonene/ H_2O_2 or limonene/TBHP = 1:2 (for hydrogen peroxide the concentrations of the reactants in the reaction mixture were as follows: limonene – about 2.8 wt%, and hydrogen peroxide about 1.6 wt% and for TBHP: limonene – about 2.9 wt%, and TBHP 1.5 wt%, respectively), methanol concentration 95 wt% and the catalyst content in the reaction mixture of 2.45 wt%. The process was carried out in a glass reactor with the capacity of 25 cm^3 , equipped with a reflux condenser, a thermometer and a magnetic stirrer. The raw materials were introduced into the glass reactor in the following order: catalyst, limonene, methanol and 60 wt% water solution of hydrogen peroxide (or TBHP). The temperature of 70°C was achieved with help of a silicon oil bath. The progress of the reaction was examined after the following reaction time: 30 min, 1 h, 1.5 h, 2 h, 2.5 h, 3 h, 4 h, 5 h, 24 h and 48 h. During the studies

also blank experiment was done and it shows that hydrogen peroxide and TBHP did not oxidize limonene without the catalyst.

Samples taken at different reaction time were analyzed by a GC-method on a Focus apparatus equipped with a flame-ionization detector and fitted with the Restek Rtx-WAX capillary column filled with polyethylene glycol. The parameter of the GC-method were as follows: helium pressure of 50 kPa, sensitivity 100, the temperature of the sample chamber 200°C , the detector temperature 250°C , and the temperature of the thermostat was increased according to the following program: isothermally at the temperature 60°C for 2 min, an increase to the temperature 240°C at the rate of $15^\circ\text{C}/\text{min}$, isothermally at the temperature 240°C for 4 min, and at the last stage cooling to the temperature 60°C . The products of limonene epoxidation were also qualitative identified by GC-MS method. The hydrogen peroxide conversion was measured by the iodometric titration method.

On the basis of mass balances the main functions describing the process of limonene oxidation were calculated: the selectivities of the appropriate products in relation to limonene consumed (L)— $S_{\text{product/L}}$, the conversion of limonene— C_L and the selectivity of transformation to organic compounds in relation to hydrogen peroxide consumed (the efficiency of hydrogen peroxide conversion)— $S_{\text{org. comp./H}_2\text{O}_2}$. The ways of the calculations these main functions are presented below:

$$S_{\text{product/L}} = \frac{\text{amount of moles of product}}{\text{amount of moles of limonene consumed}} \cdot 100(\text{mol}\%)$$

$$C_L = \frac{\text{amount of moles of limonene consumed}}{\text{amount of moles of limonene introduced into reactor}} \cdot 100(\text{mol}\%)$$

$$S_{\text{org. comp./H}_2\text{O}_2} = \frac{\text{amount of moles of formed organic compounds}}{\text{amount of moles of H}_2\text{O}_2 \text{ consumed}} \cdot 100(\text{mol}\%)$$

The samples of the FeEP catalysts used in the process of limonene oxidation were next separated from the post-reaction mixture, washed with 500 ml of the deionized water and dried at the temperature of 119°C for 5 h. After drying the FeEP catalysts were again used in the process of limonene oxidation. The oxidation was performed at the same condition as previously, but the progress of the reaction was checked only for the reaction time: 3 h and 24 h.

3. Results and discussion

3.1. X-rays diffraction analysis

[Fig. 1](#) shows X-ray diffraction patterns of the catalysts and the support. All the samples showed three distinguishable signals (002), (100) and (110), which indicated a partially graphitic structure of the support – activated carbon [26]. These signals are very broad and the peak (004), (101) and (006), typical for high graphitized carbons [27], are not observed. The degree of graphitization activated carbon EP is not high.

No additional peaks were observed in the XRD pattern of the catalyst contained 0.68 wt% of iron. The XRD pattern of catalyst contained 2.64 wt% of Fe shows additional, quite sharp peaks at 30.06° , 35.41° , 53.38° , 56.90° , 62.49° , and 89.54° which indicate that cubic Fe_3O_4 was formed. The signals of (002) and (100) were slightly changed because of the reflections at 18.28 , 43.03 characteristic for cubic Fe_3O_4 . Very slight peak at 35.41° (the strongest signal of cubic Fe_3O_4) can be observed in the XRD pattern of catalyst contained 1.32 wt% of iron. Both Fe^{2+} and Fe^{3+} were present in the catalyst.

The microcrystalline structural parameters of the catalysts support are presented in [Table 1](#). It is worth to say that, the calculated

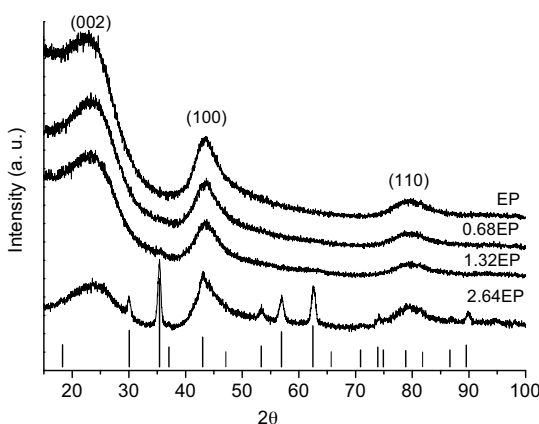


Fig. 1. X-ray diffraction patterns of the catalysts and the support. The vertical bars shows position intensity of diffraction patterns of Fe₃O₄ (JCPDS: 19-0629).

Table 1

Microcrystalline structural parameters of the catalysts support.

Catalyst	<i>d</i> (nm)	<i>L_c</i> (nm)	<i>L_a</i> (1 0 0)	<i>L_a</i> (1 1 0)	<i>L</i> (nm)	<i>n_l</i>
EP	0.375	1.17	3.41	3.38	2.2	3.1
0.86EP	0.372	1.09	3.5	3.46	2.18	2.9
1.32EP	0.37	1.07	3.56	3.48	2.19	2.9
2.64EP	0.367	1.03	4.11	4	2.37	2.8

L_c and *L_a* values are not exactly equal to the stacking height and lateral size of the crystallites because this method was developed for highly graphitized carbons. For fully disordered carbons method can be used as convenient relative estimates. The real values of crystallite sizes are probably slightly higher.

The interlayer spacing of the support is equal to 0.375 nm and is higher than typical graphitic dimensions of 0.335 nm. The interlayer spacing value is very similar to results found in literature for other activated carbons [28,29]. The numbers of layers per stack is about 3. This observation indicates that support is composed of fully disordered structures. The addition of Fe₂O₃ slightly decreases the interlayer spacing. Small increase in the crystallite height (*L_c*) and a small decrease in the lateral crystallite dimension (*L_a*), is also observed.

On the basis of Scherrer's equation the average crystallite size of Fe₃O₄ was calculated to be 14 nm.

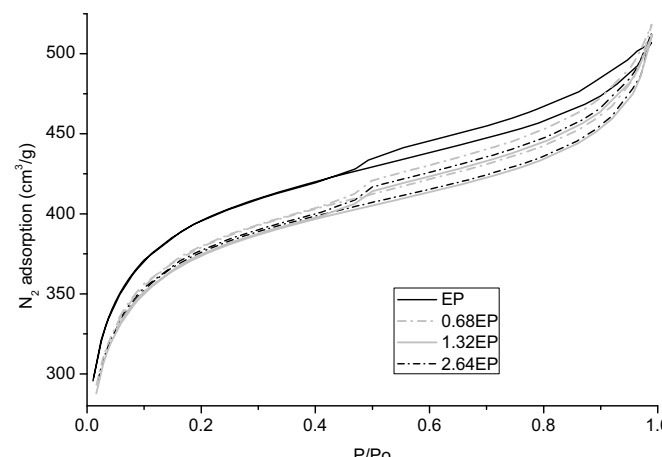


Fig. 2. Nitrogen sorption isotherms of the samples.

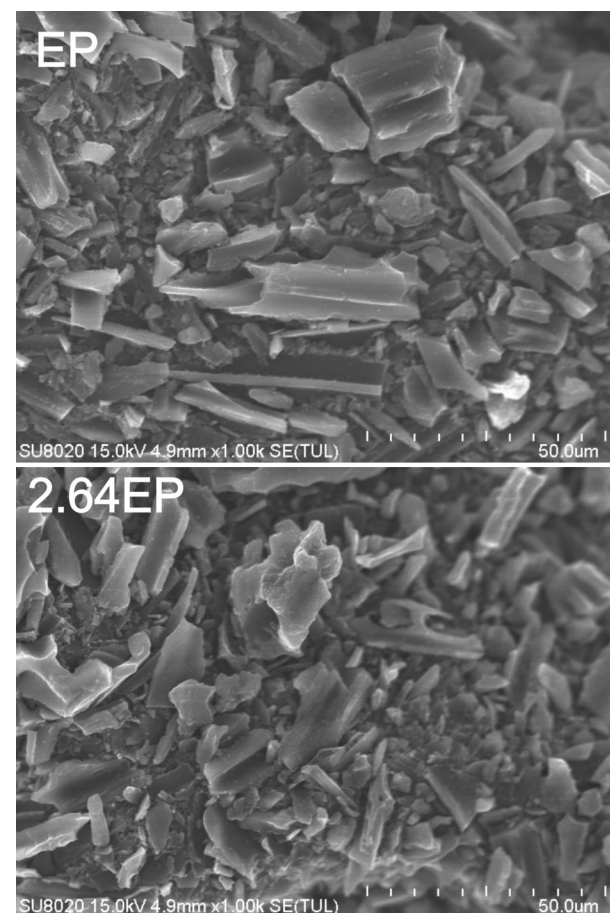


Fig. 3. FE-SEM image of the support and catalyst containing 2.64 wt% Fe, magnification by 1000 times.

3.2. Specific surface area and pore structure analysis by using nitrogen sorption

Fig. 2 shows nitrogen sorption isotherm of the catalysts and support. All the isotherms are similar. The high adsorption capacity at low partial pressure, hysteresis loop, and limiting uptake over a range of high *p/p⁰* is observed. It indicates a combination of a type I isotherm with a type IV isotherm according to UPAC classification [30] characteristic for microporous–mesoporous materials.

Hysteresis is usually associated with capillary condensation in mesopore structures. Hysteresis loops start from the relative pressure equal to 0.5. On the basis of hysteresis loop shape (parallel and nearly horizontal branches) was found that materials exhibited type H4 hysteresis loops. Type H4 loop is associated with narrow slit-like pore.

Table 2 shows the textural parameters of the samples. The addition of the small amount of Fe₃O₄ cause slight decrease of the specific surface area, total pore volume and micropore volume while the further addition of Fe₃O₄ has no effect on these parameters. On the basis on the above findings, we conclude only

Table 2

The textural parameters of the samples.

Sample	S _{BET} (m ² /g)	TPV (cm ³ /g)	MPV (cm ³ /g)
EP	1485	0.802	0.561
0.68EP	1420	0.794	0.535
1.32EP	1413	0.792	0.531
2.64EP	1416	0.793	0.535

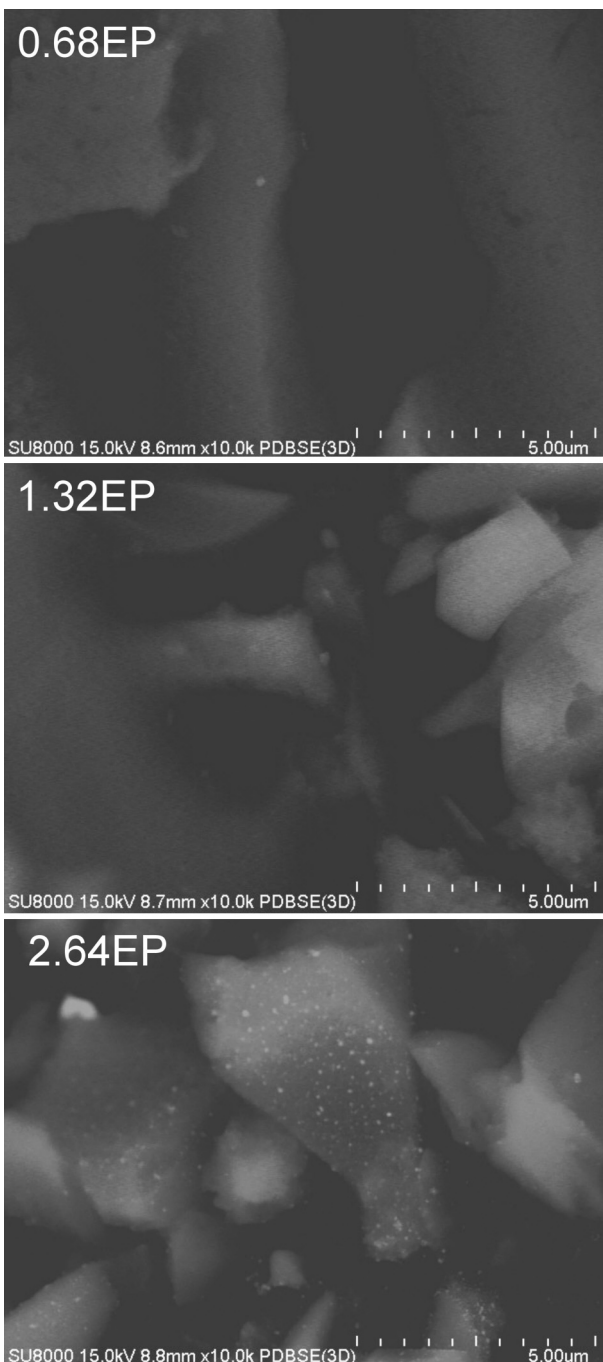


Fig. 4. FE-SEM images of the catalysts, PD-BSE detector, magnification by 1000,000 times.

insignificant amounts of iron(II,III) oxide are able to migrate inside pores.

3.3. The Field Emission Scanning Electron Microscopy (FESEM) and Energy-dispersive Spectrometer (EDS) analysis

The morphology of the catalysts was investigated by FE-SEM method. On the basis on FE-SEM micrographs using secondary electron (SE) detectors was found that EuroPh is coarse grained activated carbon with oblong grain dimensions of 10–50 μm (Fig. 3).

The support and the catalyst containing 2.64% Fe are presented in Fig. 3. The shape and size of support does not change after active phase deposition. The micrographs of 0.68EP and 1.32EP are similar.

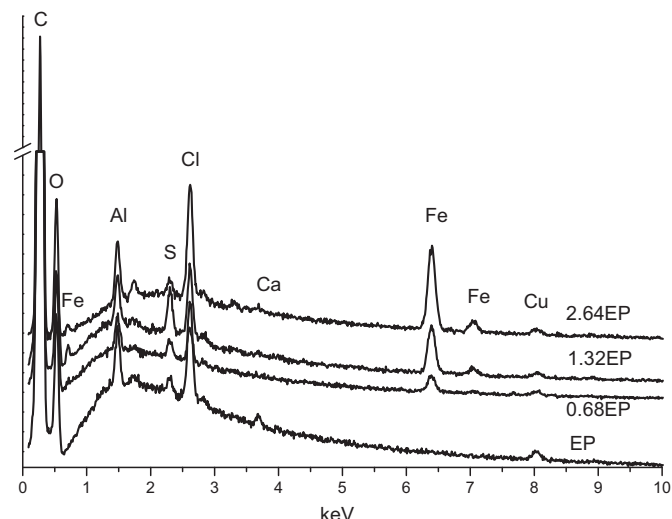


Fig. 5. The EDS spectrum of the samples.

The backscattered electron images of the catalysts are illustrated in Fig. 4 and shows the presence of bright particles sticking to the surface. The PD-BSE image is used to illustrate the distribution of iron. Only one Fe particle is present at the micrographs of 0.68EP. A few Fe particles are seen on the surface of 1.32EP. A lot of scattered Fe particles are observed on the 2.64EP.

The EDS spectrum of a support catalyst shows only peaks for carbon, oxygen aluminum, sulfur, chlorine, calcium, cuprum (Fig. 5). Iron was not detected. The peaks of Fe appear in all the catalyst. The iron contents on the surface were estimated with an accuracy of one decimal place and are presented in Table 3. The difference between Fe concentration in the catalyst and Fe concentration on the surface was 0.3 wt% for all the materials. Only about 0.4–0.5 g Fe₂O₃ per 100 g of support is placed inside pores. This conclusion is consistent with the results of the nitrogen sorption studies.

3.4. Determination of iron content by the ICP-AES method

The Fe concentration in catalyst was estimated by ICP-AES method. The iron contents were as follows: 0.85, 1.32, 3.64 wt%.

While we have not found the K_α emission of Fe in the EDS spectra of the support–EuroPh, we examined the content of iron by a technique with a lower detection limit. For this purpose, we used the ICP-AES technique. On the basis of the ICP-AES analysis we have found a content of Fe in a EuroPh equal to 1.9 × 10⁻⁴ wt%. In a typical reaction, about 0.09–0.160 g of the catalyst was used. Taking into account trace amounts of iron in the support and the small amount of EuroPh used in the reaction and is obvious that the probability of the iron contribution to the oxidation on EuroPh is not high. Similar conclusion was arrived by Bonon et al. [31]. These authors applied 0.1 g of the alumina catalyst with Fe content of 5.6 × 10⁻³ wt%.

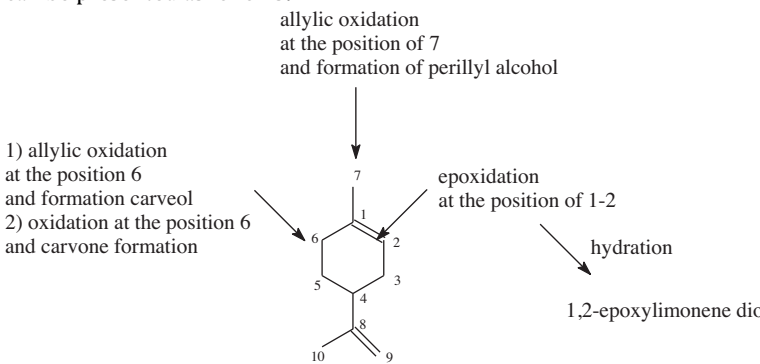
Table 3
The iron content on the surface of the catalyst estimated by EDX method.

Catalyst	Fe wt% from EDX	Difference*
0.68EP	0.4	0.3
1.32EP	1.0	0.3
2.64EP	2.3	0.3

* Difference between Fe content in catalyst and Fe content estimated by EDX rounded one decimal place.

3.5. The studies on the activity of the obtained Fe/EuroPh catalysts in the epoxidation of limonene with hydrogen peroxide

The preliminary studies on the epoxidation of limonene with hydrogen peroxide described by Wróblewska [32] showed that various directions of the oxidation of limonene molecule are possible. According to this work the general ways of the limonene oxidations can be presented as follows:



The studies on the activity of the Fe/EuroPh catalysts (0.68EP, 1.32EP and 2.64EP) showed that all catalysts were active in the oxidation process but their activity was not always the same. It was observed for 0.68EP and 1.32EP catalysts that first products of the oxidation reaction were detected in the reaction mixture only after 5 h of reaction performing (1,2-epoxylimonene diol, carvone and perillyl alcohol). In case of 0.68EP catalyst, the conversion of limonene increased from 25 mol% (5 h) to 82 mol% (48 h) and the efficiency of hydrogen peroxide conversion was very high and amounted to about 97 mol% in the range of reaction time from 5 to 48 h. In case of 1.32EP catalyst also the same first products of reaction were observed only after 5 h of reaction performing. The conversion of limonene increased from 25 mol% (5 h) to 37 mol% (48 h) and the efficiency of hydrogen peroxide conversion from 84 mol% (5 h) to 90 mol% (5–48 h). Taking into account the values of the conversion of limonene and the efficiency of hydrogen peroxide conversion the highest activity from the studied catalysts showed the 2.64EP catalyst. First products were detected after 1 h of reaction conducting (1,2-epoxylimonene diol, and perillyl alcohol). The conversion of limonene raised from 19 mol% (1 h) to 100 mol% (48 h), and the efficiency of hydrogen peroxide conversion from 47 mol% (1 h) to 55 mol% (48 h). It shows that the last studied catalyst was also very active in ineffective decomposition of hydrogen peroxide in comparison to 0.68EP and 1.32EP catalysts.

The values of the selectivities of the appropriate products obtained during the studies on the oxidation of limonene with hydrogen peroxide over the Fe/EuroPh catalysts are presented on Figures: 0.68EP (Fig. 6), 1.32EP (Fig. 7) and 2.64EP (Fig. 8).

Figs. 6 and 7 show that for the 0.68EP and 1.32EP catalysts the formation of 1,2-epoxylimonene diol, carvone and perillyl alcohol was observed but perillyl alcohol was always the main product of the process (perillyl alcohol is the product of the allylic oxidation at the position 7 in the limonene molecule) and did not undergo further oxidative dehydrogenation to aldehyde and acid. For the 0.68EP catalysts carvone was formed with a little greater selectivity than 1,2-epoxylimonene diol and for 1.32EP catalyst this situation was opposite (1,2-epoxylimonene diol was formed with higher selectivity). The examinations allow to conclude that the obtained 1,2-epoxylimonene (the product of the epoxidation at the position 1–2 in the limonene molecule) was unstable in the reaction condition and very easy underwent transformation to its diol (the reaction of hydration of the epoxide ring). The obtained results also showed that the oxidation of limonene at the position 6 and formation carvone was more preferable than allylic oxidation at this position and carveol formation.

For the 2.64EP catalyst (Fig. 8) only two products were observed in the reaction mixtures (1,2-epoxylimonene diol and perillyl alcohol). The main product of the process was always 1,2-epoxylimonene diol independent of the reaction time. It shows that increasing the content of Fe in the studied catalysts causes the decrease in the tendency to allylic oxidation at the position 6 and

also a little in the tendency to the allylic oxidation in the position of 7.

The used FeEP catalysts were recovered from the post reaction mixtures and again used in the process of limonene oxidation with hydrogen peroxide. The obtained results are presented in Table 4.

Table 4 shows that over the reused catalysts the epoxidation at the position 1,2 practically did not undergo and in the reaction mixtures were observed only: carvone, carveol and perillyl alcohol. The analysis of the results concerning carveol and carvone also reveals that in contrast to the results obtained in the first run, next to carvone also carveol was obtained. Moreover, in some cases the allylic oxidation of the position 6 and carveol formation underwent more preferable than the direct oxidation at this position and carvone formation. Also conversion of limonene and efficiency of hydrogen peroxide conversion took considerably lower values. We can assumed that, the considerable decrease of the activity of the studied catalysts is connected with: the leaching of Fe from the structures, with the changes in the structure of EuroPh carrier and also with the presence of oligomers (tars).

3.6. The studies on the activity of the obtained Fe/EuroPh catalysts in the epoxidation of limonene with TBHP

The studies on the oxidation of limonene with TBHP show that the catalysts were active after a very similar time as it was observed for the studies with hydrogen peroxide.

For the 0.68EP catalyst the conversion of limonene raised from 15 mol% (5 h) to 21 mol% (48 h) and these values were considerably lower than values for oxidation with hydrogen peroxide. The same situation was observed for 1.32 FeEP catalyst. For this catalyst the conversion of limonene amounted to 7 mol% for the reaction time 4 h and 24 mol% for the reaction time 48 h. For the 2.64EP catalyst the conversion of limonene raised from 2 mol% (1.5 h) to 46 mol% (48 h) and the values of this function of the process was similar to obtained during the studies with hydrogen peroxide.

The values of the selectivities of the appropriate products obtained during the studies on the oxidation of limonene with TBHP over the Fe/EuroPh catalysts are presented on Figures: 0.68EP (Fig. 9), 1.32EP (Fig. 10) and 2.64EP (Fig. 11).

Figs. 9 and 10 show that over the 0.68EP and 1.32EP catalysts the main product was perillyl alcohol which was formed with the selectivity of about 66–77 mol%, depending on the reaction time.

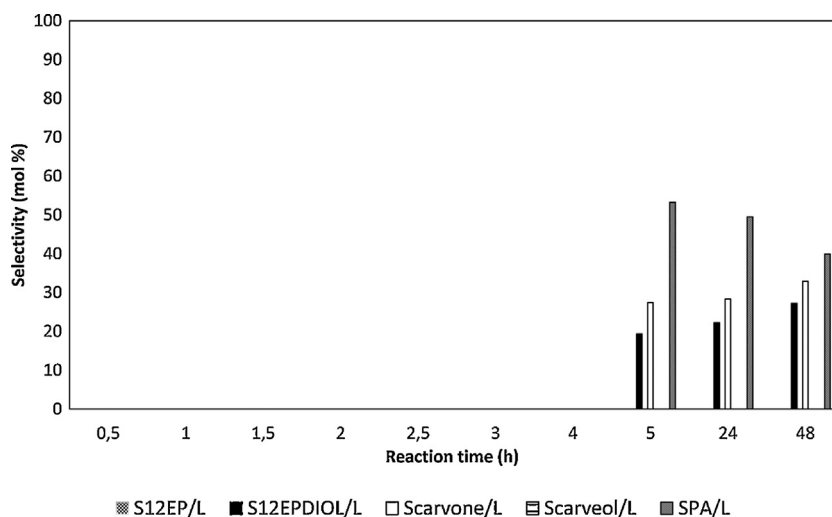


Fig. 6. The dependence of the selectivities of the main products of limonene oxidation with hydrogen peroxide over the 0.68EP catalyst: (12EPL—1,2-epoxylimonene, 12EPLDIOL—1,2-epoxylimonene diol and PA—perillyl alcohol) on the reaction time.

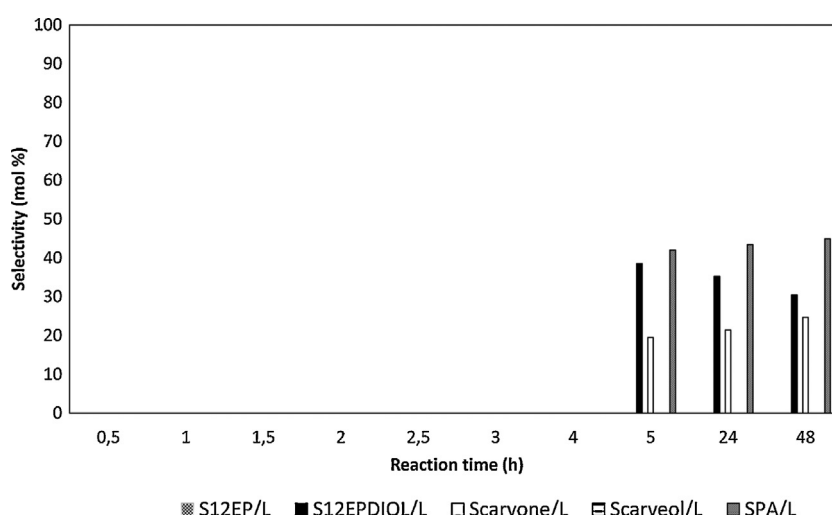


Fig. 7. The dependence of the selectivities of the main products of limonene oxidation with hydrogen peroxide over the 1.32EP catalyst: (12EPL—1,2-epoxylimonene, 12EPLDIOL—1,2-epoxylimonene diol and PA—perillyl alcohol) on the reaction time.

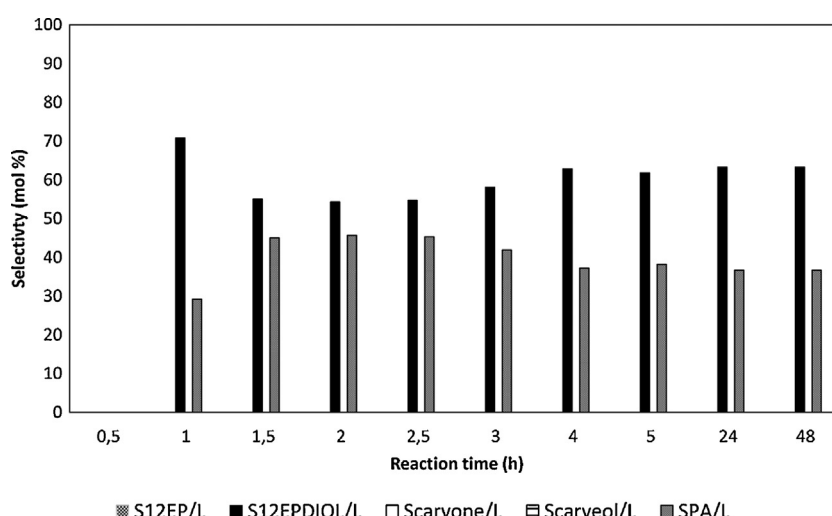


Fig. 8. The dependence of the selectivities of the main products of limonene oxidation with hydrogen peroxide over the 2.64EP catalyst: (12EPL—1,2-epoxylimonene, 12EPLDIOL—1,2-epoxylimonene diol and PA—perillyl alcohol) on the reaction time.

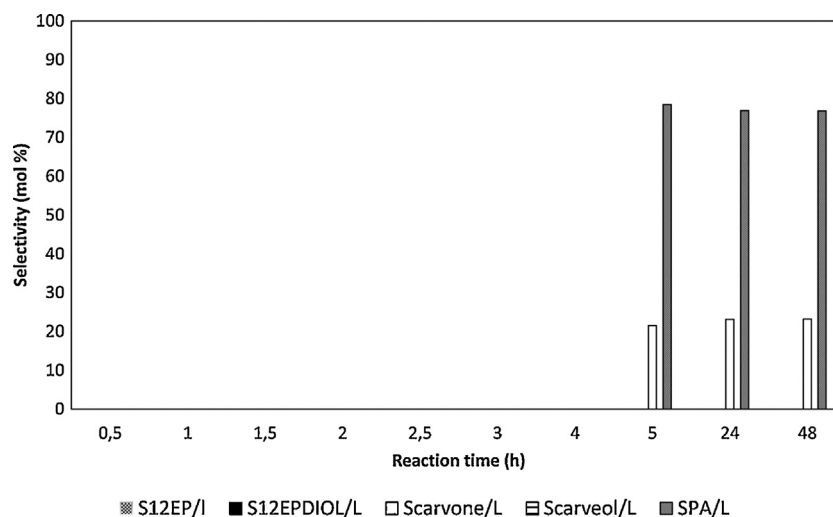


Fig. 9. The dependence of the selectivities of the main products of limonene oxidation with TBHP over the 0.68EP catalyst: (12EPL—1,2-epoxylimonene, 12EPLDIOL—1,2-epoxylimonene diol and PA—perillyl alcohol) on the reaction time.

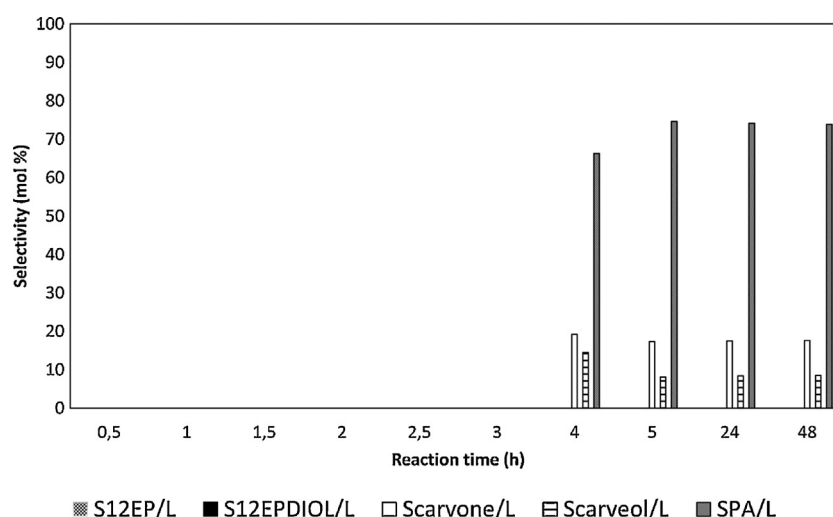


Fig. 10. The dependence of the selectivities of the main products of limonene oxidation with TBHP over the 1.32EP catalyst: (12EPL—1,2-epoxylimonene, 12EPLDIOL—1,2-epoxylimonene diol and PA—perillyl alcohol) on the reaction time.

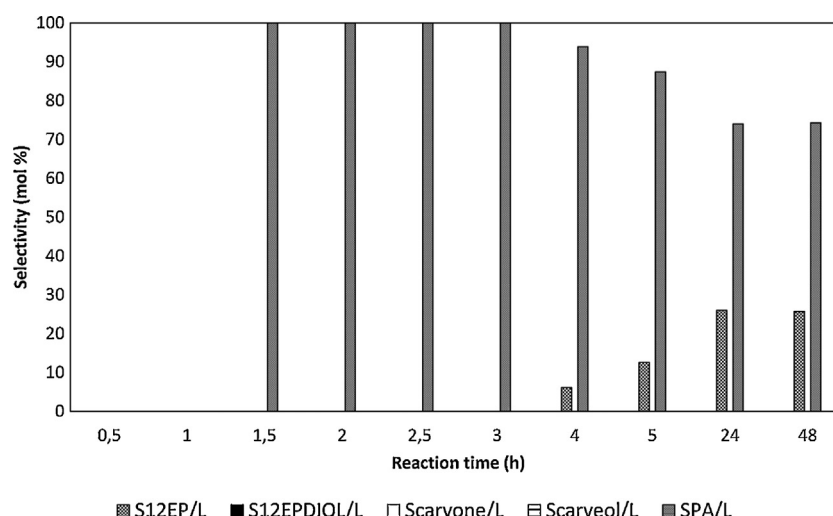


Fig. 11. The dependence of the selectivities of the main products of limonene oxidation with TBHP over the 2.64EP catalyst: (12EPL—1,2-epoxylimonene, 12EPLDIOL—1,2-epoxylimonene diol and PA—perillyl alcohol) on the reaction time.

Table 4

The results the examination of the recovered FeEP catalysts in the oxidation of limonene with hydrogen peroxide (in the braces are given for comparison the values for the fresh catalysts).

Reaction time (h)	$S_{12EP/L}$ (mol%)	$S_{12EPDIOL/L}$ (mol%)	$S_{carvone/L}$ (mol%)	$S_{carveol/L}$ (mol%)	$S_{PA/L}$ (mol%)	C_L (mol%)	$S_{org. comp./H_2O_2}$ (mol%)
0.68EP							
3	0 (0)	0 (0)	26 (0)	74 (0)	0 (0)	3 (0)	16 (0)
24	0 (0)	0 (22)	37 (28)	20 (0)	43 (50)	16 (50)	42 (99)
1.32EP							
3	0 (0)	0 (0)	0 (0)	0 (0)	0 (0)	0 (0)	0 (0)
24	0 (0)	4 (35)	20 (21)	42 (0)	34 (43)	21 (30)	32 (90)
2.64EP							
3	0 (0)	0 (58)	28 (0)	72 (0)	0 (42)	4 (65)	60 (51)
24	0 (0)	0 (63)	19 (0)	42 (0)	38 (37)	10 (100)	28 (55)

Table 5

The results the examination of the recovered FeEP catalysts in the oxidation of limonene with TBHP (in the braces are given for comparison the values for the fresh catalysts).

Reaction time (h)	$S_{12EP/L}$ (mol%)	$S_{12EPDIOL}$ (mol%)	$S_{carvone/L}$ (mol%)	$S_{carveol/L}$ (mol%)	$S_{PA/L}$ (mol%)	C_L (mol%)
0.68EP						
3	0 (0)	0 (0)	0 (0)	100 (0)	0 (0)	1 (0)
24	0 (0)	0 (0)	0 (23)	100 (0)	0 (77)	3 (17)
1.32EP						
3	0 (0)	0 (0)	0 (0)	100 (0)	0 (0)	1 (0)
24	0 (0)	0 (0)	0 (23)	100 (0)	0 (77)	5 (17)
2.64EP						
3	0 (0)	0 (0)	0 (0)	100 (0)	0 (100)	1 (19)
24	0 (26)	0 (0)	0 (0)	100 (0)	0 (74)	2 (46)

The formation of 1,2-epoxylimonene over these catalysts was not observed. The second direction of the limonene oxidation over these catalysts was the direct oxidation at the position 6, and carvone formation. In case of 1.32EP catalyst also formation of carveol was observed but with small selectivity 8–15 mol%. Similar to the studies over the 2.64EP catalysts with hydrogen peroxide, during the studies with TBHP the formation of product of allylic oxidation at position of 6 was not observed (Fig. 11). For this sample only perillyl alcohol and 1,2-epoxylimonene were detected in the reaction mixture, but for the reaction time 13–3 h perillyl alcohol was the only product of the oxidation.

The used FeEP catalysts were recovered from the post reaction mixtures and again used in the process of limonene oxidation with TBHP. The obtained results are presented in Table 5. Table 5 shows that reused catalyst had very low activity in the oxidation of limonene, independent of the Fe content. The only one product of the process was perillyl alcohol which was formed at the conversion of limonene amounted to about 1–5 mol%, even for the reaction time 24 h.

4. Conclusions

The studies showed that all obtained catalysts (0.68EP, 1.32EP and 2.64EP) were active catalysts the oxidation of limonene with hydrogen peroxide and *t*-butyl hydroperoxide, and the main product of this oxidation was perillyl alcohol (allylic oxidation at position 7 in limonene molecule). For the oxidation with hydrogen peroxide also epoxidation of the unsaturated bond in the position 1–2 in the limonene molecule was observed and further hydration this compound to diol. During the studies with TBHP 1,2-epoxylimonen was obtained only for studies with 2.63EP, but with low selectivity. For the catalysts with the lowest Fe content (0.68EP and 1.32EP) independent of the used oxidant, formation of carvone was observed. This compound was obtained as a result of the direct oxidation of limonene molecule at the position 6. Carveol, the product of allylic oxidation at the position 6 was detected in the reaction mixture only for 1.32EP during the studies with TBHP. Over the other studied catalysts the allylic oxidation at the position 6 was

not observed, independent of the used oxidizing agent. The reused catalysts lost considerably their activity, it was especially visible for the studies with TBHP. Taking into account the promising results obtained during the studies on the utilization of Fe/EuroPh catalysts in limonene oxidation, these catalysts can be recommended for consideration by researchers from the organic chemical industry.

References

- [1] H.J. Bouwmeester, M.C.J.M. Konings, J. Gershenson, F. Karp, R. Croteau, *Phytochemical* 50 (1999) 243.
- [2] K.S. Suslick, B.R. Cook, *J. Chem. Soc., Chem. Commun.* (1987) 200–202.
- [3] R.A. Sheldon, J.K. Kochi, *Metal-Catalysed Oxidations of Organic Compounds*, Academic Press, New York, NY, 1981.
- [4] R.A. Sheldon, *J. Mol. Catal. A: Chem.* 20 (1983) I–I26.
- [5] M. de Fatima Teixeira Games, O.A.C. Antunes, *J. Mol. Catal. A: Chem.* 121 (1997) 145–155.
- [6] J. Li, Z. Li, G. Zi, Z. Yao, Z. Luo, Y. Wang, D. Xue, B. Wang, J. Wang, *Catal. Commun.* 59 (2015) 233–237.
- [7] C.K. Modi, J.A. Chudasama, H.D. Nakum, D.K. Parmar, A.L. Patel, *J. Mol. Catal. A: Chem.* 395 (2014) 151–161.
- [8] L.S. Yuan, J. Efendi, N.S.H. Razali, H. Nur, *Catal. Commun.* 20 (2012) 85–88.
- [9] M. Abrantes, S.M. Bruno, C. Tome, M. Pillinger, I.S. Goncalves, A.A. Valente, *Catal. Commun.* 15 (2011) 64–67.
- [10] A.J. Bonon, D. Mandelli, O.A. Kholdeeva, M.V. Barmatova, Y.N. Kozlov, G.B. Shulpin, *Appl. Catal. A: Gen.* 365 (2009) 96–104.
- [11] P. Oliveira, A. Machado, A.M. Ramos, I. Fonseca, F.M. Braz Fernandes, A.M. Botelho do Rego, *J. Vital, Microporous Mesoporous Mater.* 120 (2009) 432–440.
- [12] P. Oliveira, A. Machado, A.M. Ramos, I.M. Fonseca, F.M. Braz Fernandes, A.M. Botelho do Rego, *J. Vital, Catal. Commun.* 8 (2007) 1366–1372.
- [13] P. Oliveira, M.L. Rojas-Cervantes, A.M. Ramos, I.M. Fonseca, A.M. Botelho do Rego, *J. Vital, Catal. Today* 118 (2006) 307–314.
- [14] J.-F. Bartoli, K. Le Barch, M. Palacio, P. Battioni, D. Mansuy, *Chem. Commun.* (2001) 1718–1719.
- [15] D. Naróg, A. Szczepanik, A. Sobkowiak, *Catal. Lett.* 120 (2008) 320–325.
- [16] M. Caovilla, A. Caovilla, S.B.C. Pergher, M.C. Esmelindro, C. Fernandes, C. Dariva, K. Bernardo-Gusmao, E.G. Oestreicher, O.A.C. Antunes, *Catal. Today* 133–135 (2008) 695–698.
- [17] I.Y. Skobelev, E.V. Kudrik, O.V. Zalomaeva, F. Albrieux, P. Afanasyev, O.A. Kholdeeva, A.B. Sorokin, *Chem. Commun.* 49 (2013) 5577–5579.
- [18] M. Madadi, R. Rahimi, *Reac. Kinet. Mech. Catal.* 107 (2012) 215–229.
- [19] K. Hasan, N. Brown, C.M. Kozak, *Green Chem.* 13 (2011) 1230–1237.
- [20] B.S. Lane, K. Burgess, *Chem. Rev.* 103 (2003) 2457–2473.
- [21] P. Scherrer, *Nachr. Ges. Wiss. Gottingen* 2 (1918) 98–100.
- [22] J. Ziebro, B. Skorupińska, G. Kądziołka, B. Michalkiewicz, *Fullerenes Nanotubes Carbon Nanostruct.* 21 (2013) 333–345.

- [23] J. Randall, H.P. Rooksby, B.S. Cooper, Z. Kristallogr. 75 (1930) 196–214.
- [24] B.E. Warren, Phys. Rev. 59 (1941) 693–698.
- [25] F.G. Emmerich, C.A. Luengo, Carbon 31 (1993) 333–339.
- [26] X. Qi, B. Blizanac, A. DuPasquier, P. Meister, T. Placke, M. Oljaca, J. Li, M. Winte, Phys. Chem. Chem. Phys. 16 (2014) 25306–25313.
- [27] J. Zhao, L. Yang, F. Li, R. Yu, C. Jin, Carbon 47 (2009) 744–751.
- [28] B.S. Grgis, Y.M. Temerk, M.M. Gadelrab, I.D. Abdullah, Carbon Sci. 8 (2007) 95–100.
- [29] J. Sreńcek-Nazzal, W. Kamińska, B. Michalkiewicz, Zvi C. Koren, Ind. Crops Prod. 47 (2013) 153–159.
- [30] K.S.W. Sing, D.H. Everett, R.A.W. Haul, L. Moscou, R.A. Pierotti, J. Rouquerol, T. Siemieniewska, Pure Appl. Chem. 57 (1985) 603–619.
- [31] A.J. Bonon, Y.N. Kozlov, J.O. Bahú, R.M. Filho, D. Mandelli, G.B. Shulpin, J. Catal. 319 (2014) 71–86.
- [32] A. Wróblewska, Molecules 19 (12) (2014) 19907–19922.